CHARACTERIZING DYNAMIC EFFECTS OF OSCILLATOR POWER CYCLING

D. A. Howe, D. Lirette, N. Ashby, A. Hati, and C. Nelson
Time and Frequency Division, NIST, Boulder, CO, USA
Email: *dhowe@nist.gov*

Abstract

We create a measurement technique and easy to interpret metrics to be used in development of new oscillators specifically for applications in which the oscillator's power is turned on and off. This is useful in predicting the performance in, for example, the frequency-difference-of-arrival (FDOA) geolocation technique, which is used to monitor and track an emitter's location by observing its Doppler frequency shifts at a set of receivers. To conserve energy, FDOA applications compute Doppler tracks from an emitter that is powered "on" or measured for short periods (τ_{on}) after a long "off" period, called the "stride" interval (τ_s). For lowest size, weight, and power (SWaP) and lowest phase noise and best frequency stability, evaluations are focused on Oven-Controlled Crystal Oscillators (OCXO's) and Temperature-Controlled Crystal Oscillators (TCXO's). For illustration, we use τ_{on} = 3 s and τ_s = 60 s. This shows the need to consider the dynamic behavior during the short 3 s average frequency measurements as well as the 60 s sampling interval between measurements. Dynamic Allan Deviation (ADEV) does not accurately capture different noise types for such a short 3 s sample, so we propose using Dynamic ThêoH which characterizes the oscillator at power-on more accurately. Since RMS frequency differences vs. sampling time-intervals in multiples of 60 s cannot be used in place of the ADEV, we regard frequency differences as an uncertainty on an oscillator's predicted frequency, not on a mean frequency. This mimics ADEV and we can distinguish the dominant component of frequency prediction due to random-walk FM (RWFM) or an even more divergent noise type. This paper: (1) describes a measurement setup to obtain low-noise, fast fractional-frequency, time-series measurements, (2) motivates and illustrates Dynamic ThêoH, the hybrid of ADEV and THEO, for τ_{on} = 3 s, (3) constructs a statistic called $Y(\tau_{on},\tau_s)$ which estimates a τ_s = 60 s frequency prediction error, and (4) transforms 3 s time-series measurements to phase noise L(f) for field applications and evaluations.

I. INTRODUCTION AND SUMMARY

We characterize an oscillating signal for applications where the oscillator is either only "on" or measured for short periods (τ_{on}) during long, periodic or "stride" intervals (τ_s), during which the oscillator is off for τ_s- τ_{on} seconds. A statistic called Psi-deviation, $\Psi(\tau_{on},\tau_s)$, is created, which estimates the frequency prediction error using the last frequency measurement. The variance of the prediction is $\Psi^2(\tau_{on},\tau_s)$, which is a time-averaged, two-sample variance and provides desirable properties similar to the Allan variance. The application is the tracking of an emitter using frequency difference of arrival (FDOA). While the emitter's oscillating signal is on and transmitting (or being measured), receivers calculate tracks based on Doppler shifts that in turn provide a navigation solution. On a 2-dimensional plane, circular error probability (CEP) due to the emitter's oscillator noise is minimized given low enough phase noise and frequency error during the interval τ_{on}. Because τ_{on} is short, and we want to optimally characterize

Authors are with the National Institute of Standards and Technology, Boulder, CO 80305 USA.

frequency stability, we compute ThêoH **[1]**. Using 10 sequential segments of τ_{on}, we display each segment's ThêoH in a "waterfall" or surface plot, to characterize the oscillator's turn-on transient. Dubbed "Dynamic ThêoH", or DThêoH, we can compare how long it takes different oscillators to obtain consistent ThêoH. Oscillators having low enough cost, size, weight, and power appropriate for power cycling are OCXOs and TCXOs, or oven and temperature compensated MEMs oscillators, respectively. Section II details the measurement setup and an example of DThêoH for an OCXO. Section III motivates and develops frequency prediction error $\Psi(\tau_{on}, \tau_s)$. Section IV derives the relationship between Ψ-variance in the time domain and spectral density $S_y(f)$. Sections V and VI show time-domain and frequency-domain measurements, respectively, comparing an OCXO and TCXO in limited live-time operation.

II. DYNAMIC THÊOH WHILE OSCILLATOR IS ON

We want to capture oscillator turn-on frequency stability and establish the dynamic ADEV as a useful format for characterizing the oscillator's behavior **[2]**. ThêoH is preferred rather than ADEV when an oscillator is on for only a short period compared to its off-time. ThêoH is a hybrid (hence the "H") of ADEV for short-term averaging times plotted with a bias-removed version of Thêo1, called ThêoBR **[3]** for long term. The Thêo portion characterizes to 75% of a data run, whereas straight ADEV characterizes to only 20% **[1]**. To illustrate, ThêoH plots are generated from measurements for the oscillators tested while powered on for a data run of only three-second duration. Fig. 1 shows the measurement setup. Dynamic ThêoH is a waterfall graph where each 3 s run is parsed into ten sequential time segments, then ThêoH is computed for each segment and displayed as another waterfall plot, as shown in Fig. 2.

Such plots provide a quick assessment of how long and to what degree it takes an oscillator to settle down to a consistent stability after being turned on.

We will use an example in which the emitter is repeatedly turned on for 3 s every 60 s. In addition to the frequency that is traced during start-up, discussed above, an important criterion is the start-up frequency reproducibility and its characterization, described next.

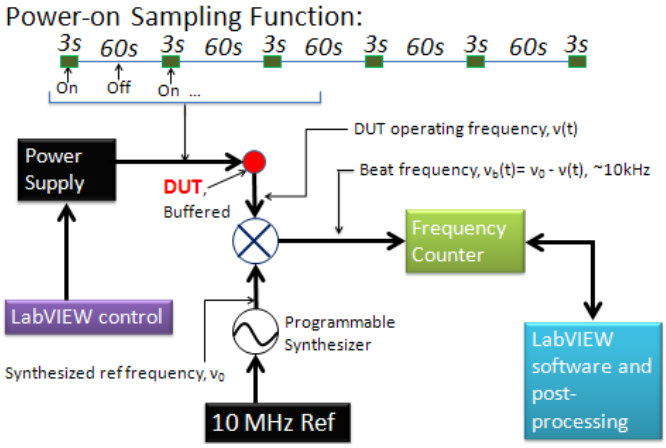

Figure 1. The device-under-test (DUT) is a temperature compensated oscillator with quartz or MEMs resonator.

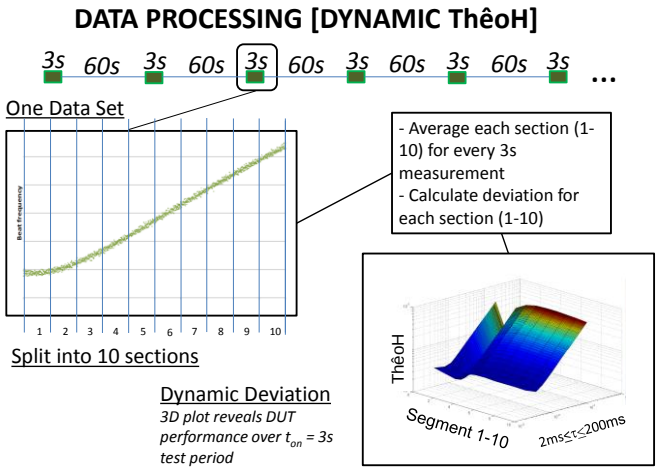

Figure 2. Dynamic ThêoH plot. Surface smoothness is a general measure that the test oscillator has attained steady-state operation after having been powered on.

III. FREQUENCY PREDICTION ERROR FOR MULTIPLES OF τ_s

We wish to estimate an oscillator's frequency at its next turn-on. While there are any number of different ways to make this estimate based on a history of actual measurements **[4]**, we construct a 2-sample frequency prediction to mimic the desirable properties of noise identification, convergence, convenience, and acceptance provided by the 2-sample standard variance, better known as the Allan variance, and its square root, ADEV **[5]**. The two-sample, no dead-time Allan variance has widely accepted statistical properties; however, limited-live applications have substantial dead time.

Fractional-frequency error $y_{on}(t)$ and its prediction at $y_{on}(t+\tau_s)$ is based on the reasonable assumption that any given manufacturer wants $y_{on}(t+\tau_s)$ to be the same value as measured values of $y_{on}(t)$. Since $y_{on}(t+\tau_s) = (1+\varepsilon)y_{on}(t)$, where ε is a random variable, we also expect the average $\frac{1}{N}\sum_{n=1}^{N} y_{on}(t-n\tau_s)$ to be dependent on N, i.e. nonstationary, without a central limit, thus, unfortunately of little or no practical use in the estimate (designated by "^" as $\hat{y}_{on}(t+\tau_s)$). The most efficient method for random-walk noise predicts that $\hat{y}_{on}(t+\tau_s) = y_{on}(t)$, the last measured value of y_{on}. The variance of this expectation can be written as a first difference:

$$\Psi^2(\tau_{on},\tau_s) = \left\langle \left[\hat{y}_{on}(t+\tau_s) - y_{on}(t)\right]^2 \right\rangle \qquad \text{Eq. 1}$$

where $\langle \cdot \rangle$ denotes an ensemble average based on first differences up of y_{on}. Like AVAR, (Eq. 1) is the variance of an increment and converges for random-walk noise.

DEFINITION: Samples of the fractional frequency-error function $y(t)$ occur at a rate f_s having an interval $\tau_0 = \frac{1}{f_s}$ (setup shown in Fig. 1). Given a sequence of fractional frequency errors $\{y_n : n=1,\ldots,M_y\}$ with a sampling period between adjacent measurements given by τ_0, we define the $m\tau_0$-average fractional-frequency deviate as

$$^{m}\overline{y}(t) \equiv \frac{1}{m}\sum_{j=0}^{m-1} y_{n-j},$$

where $y_n = y(t)$, with $n = t/\tau_0$ starting from a designated origin $t_0 = 0$. Define psi-variance from the space of all possible 2-sample increments:

$$\Psi_y^2(\tau_{on},\tau_s) \equiv \left\langle \left[{}^{\tau_{on}}\bar{y}(t) - {}^{\tau_{on}}\bar{y}(t-\tau_s) \right]^2 \right\rangle \qquad \text{Eq. 2}$$

where $\langle \cdot \rangle$ denotes an ensemble average and ${}^{\tau_{on}}\bar{y}(t)$ is the mean frequency over duration $\tau_{on} = m\tau_0$. Fig. 1, top, shows the sampling function associated with $\Psi^2(\tau_{on}, \tau_s)$ acting on $\{y_n\}$. τ_{on} is called the averaging or live interval, τ_s - τ_{on} is the oscillator's dead time. Note that $\Psi^2(\tau_{on}, \tau_s)$ becomes twice the two-point standard (Allan) variance $\sigma_y^2(\tau_s)$ if $\tau_{on} = \tau_s$.

IV. RELATIONSHIP OF $S_y(f)$ TO Ψ-VARIANCE

For computing the usual power spectrum, we start with Parceval's theorem:

$$\Psi^2(\tau_{on},\tau_s) = 4\int_{\frac{1}{2\tau_s}}^{f_h} |H(f)|^2 S_y(f)df \qquad \text{Eq. 3}$$

where H(f) is the frequency-domain response of the time-domain sampling function of $\Psi^2(\tau_{on}, \tau_s)$ shown at the top of Fig. 1. $S_y(f)$ of the emitter is multiplied by the FT squared of the sampling function to obtain $|H(f)|^2$. We obtain:

$$\Psi^2(r,\tau_{on},\tau_s) = 4\int_{\frac{1}{2\tau_s}}^{f_h} \frac{S_y(f)df}{\pi^2\tau_{on}{}^2 f^2}\left(\sin(\pi\tau_{on} f)\sin(\pi r\tau_s f)\right)^2 \qquad \text{Eq. 4}$$

where $r = t/\tau_s$ (starting from origin t_0) is a counting index r = 1,2,3… representing the r^{th} data run of 3 s duration.

The f-domain response function $|H(f)|^2$ is shown in Fig. 3. This response is +20 dB/decade, like the Allan variance for low frequencies up to the peak at $f\tau_s = ½$. There is insufficient roll-off above this peak for which white and flicker of phase noise types will cause the level of $\Psi^2(\tau_{on},\tau_s)$ to depend on f_h in (Eq. 4). This normal "picket-fence" response is not a concern as of yet, since DUT random walk FM (and drift) are likely to dominate limited-live applications, as discussed in Section III.

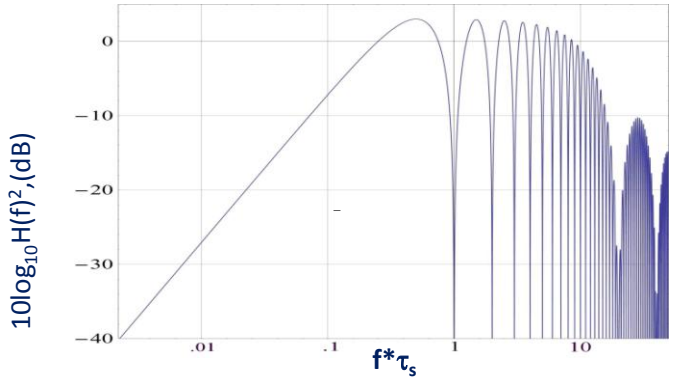

Figure 3. Frequency response $|H(f)|^2$ of $\Psi^2(\tau_{on},\tau_s)$ in (Eq. 3), $\tau_{on} = (\tau_s)/20$, $r = 1$.

White FM noise can be contributed by the measurement system at short term.

Scaling to $\frac{1}{2}\Psi^2(\tau_{on}, \tau_s)$ normalizes results to equal $\sigma_y^2(\tau_s)$ if $\tau_{on} = \tau_s$, i.e., zero dead-time. Furthermore, the zero-dead time Allan and $\frac{1}{2}\Psi^2(\tau_{on}, \tau_s)$ respond identically to White FM noise having equal frequency-spectral coefficient h_o **[6]**. Table 1 compares the transform to frequency spectrum $S_y(f)$ of $\frac{1}{2}\Psi^2(\tau_{on}, \tau_s)$ and $\sigma_y^2(\tau_s)$. Flicker noise is given in terms of $\sigma_y^2(\tau_s)$ to simplify the formula. The Table evidences the bias on $\sigma_y^2(\tau_s)$ due to limited-live operation of the DUT.

Table 1. Table of Transforms

Noise Type	Allan $\sigma_y^2(\tau)$	Psi Variance $\frac{1}{2}\Psi^2(\tau_{on}, \tau_s)$
White FM	$\frac{h_0}{2\tau}$	$\frac{h_0}{2\tau}$
Flicker FM	$2h_{-1}\log 2$	$\frac{h_{-1}}{2\tau_{on}^2}\left(\begin{array}{l} 4\tau_s\tau_{on}\tanh^{-1}\frac{\tau_{on}}{\tau_s} \\ +2\tau_{on}^2\ln\frac{\tau_s}{\tau_{on}}+ \\ (\tau_s^2+\tau_{on}^2)\ln\left(1-\frac{\tau_{on}^2}{\tau_s^2}\right)\end{array}\right)$
Random Walk FM	$\frac{2\pi^2 h_{-2}}{3}\tau$	$\frac{\pi^2 h_{-2}}{3}(3\tau_s-\tau_{on})$

We observe the intrinsic level of random-walk or drift that properly characterizes the DUT in "longer term" (as τ approaches its maximum around 2 s using ThêoH). Since fast-frequency measurements mask or are not sensitive to DUT-based PM-noise types that would appear as "super white" FM-noise in $y(t)$ raw data, $\frac{1}{2}\Psi^2(\tau_{on}, \tau_s)$ is never biased by this noise when compared to AVAR. Since it never occurs the unbiased White-FM-transform coefficient h_0, to $S_y(f)$ does not depend on a high-cutoff, $f_c = 1/(2\pi\tau_{on})$, as indicated in Table 1. Random walk (and drift) are slightly biased (depends on $r = \tau_s/\tau_{on}$ **[7]**) and the positive τ-slope is the same for $\Psi^2(\tau_{on}, \tau_s)$ and AVAR, $\sigma_y^2(\tau)$. It is important to note that flicker-FM noise using dead-time AVAR, here $\Psi^2(\tau_{on} = const., \tau_s = \tau)$, will appear as White-FM noise **[8]**.

It remains to be determined whether Flicker-FM can be reliably detected by unraveling Ψ-variance to obtain AVAR. However, this distinction is usually unimportant to Doppler-relevant applications.

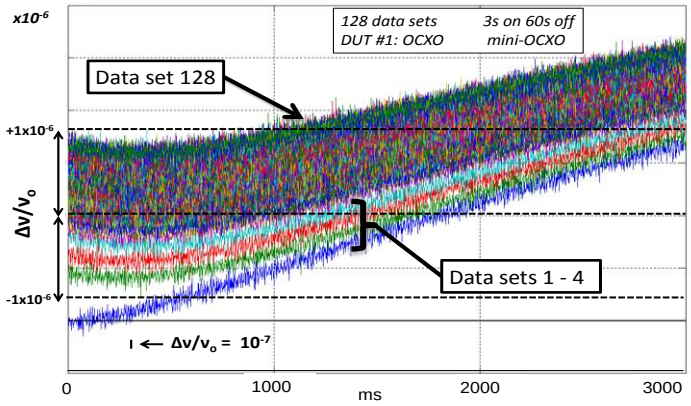

Figure 4. 128 sets of raw fractional frequency measurements. Set 1 is the first series of $y(t)$, and the oscillator is first turned on from a "cold" start. Each trace is 3 s worth of data; repeating every 60 s during which the oscillator is turned off. ν_o = 16.384MHz.

V. TIME DOMAIN MEASUREMENTS OF OSCILLATORS

We use a commercial miniature OCXO and TCXO at 16.384 and 26 MHz, respectively, as DUTs for an example. Fig. 4 shows 128 raw $y(\tau_{on})$ data runs of 2 ms sampled measurements on top of each other. At the very bottom, data set #1 starts the test oscillator. One can see that the first four sets capture a larger set-to-set overall variation than the remaining 124. In application, the oscillators are not cold-started but are in process, so the initialization sets such as 1-4 can generally be ignored. We process individual runs of Fig. 4 using dynamic ThêoH, as described in Section II. This is shown in Fig. 5 along with averages of ThêoH. One can see that a consistent level of stability (drift + White FM) is acquired after about 60 ms. Measurements are an equispaced sequence of fast-frequency errors, $y(t)$, and are not time-errors, $x(t)$. Thus, measurement noise is White FM and not typified by PM noise during runs of τ_{on}. This is not especially undesirable and Fig. 5 shows measurement White FM in short-term, i.e., $\sigma_y(\tau_0) \propto \tau^{-1/2}$.

Using the averages of each data run, $^{\tau_{on}=3s}\overline{y}(t)$, we compute $\Psi^2(\tau_{on}, \tau_s)$ using all runs. Results are shown in Fig. 6, where we observe the level and rate of frequency reproducibility as a function of $n\tau_s$ for each period in which the DUT is powered on. This level and rate may or may not limit other application-specific goals. Likewise, with a given level and rate, one may be forced to use application strategies or improve emitter reproducibility to achieve goals. Our finding is that there is no reliable method for estimating $\Psi(\tau_{on}, \tau_s)$ from $\sigma_y(\tau)$, for ADEV.

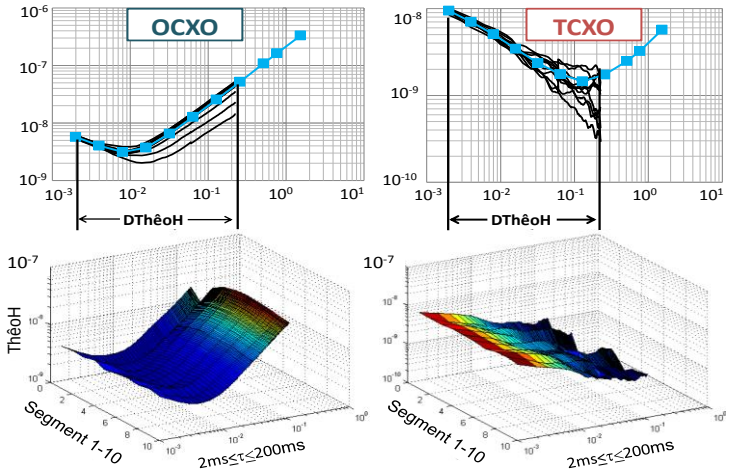

Figure 5. ThêoH deviation (top) and dynamic ThêoH (DThêoH) deviation (bottom) for the OCXO and TCXO. Note that the longest τ for DThêoH corresponds to 1/10 of the longest τ for ThêoH.

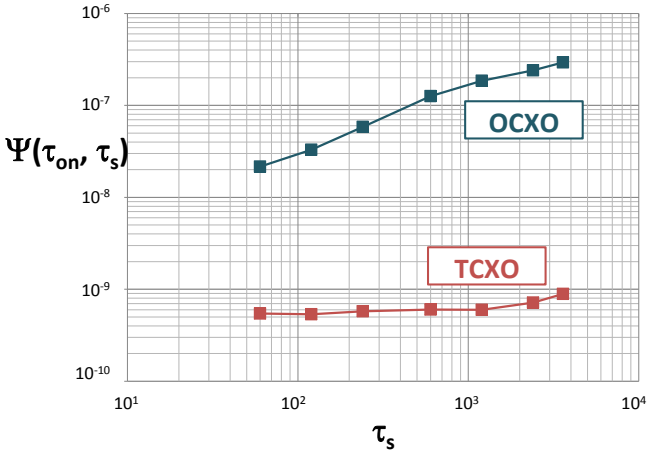

Figure 6. Ψ-deviation for an OCXO and TCXO. The minimum averaging time is τ_s = 60s.

VI. FREQUENCY DOMAIN MEASUREMENTS OF OSCILLATORS

Phase noise L(f) is important during limited-live Doppler tracking. L(f) is a convenient standard used to determine the error vs. range in offset-f, proportional to emitter velocity, as set by the emitter. L(f) is computed from the fast-frequency measurements obtained from Fig. 1. For a given τ_{on} data run sampled at t_0, the frequency spectrum $S_y(f)$ is obtained from the discrete FT of the series **[6]**:

$$Y(m\Delta f) = \frac{1}{N}\sum_{r=1}^{N} y(r\tau_0)e^{-j2\pi m\Delta f r\tau_0} \qquad \text{Eq. 5}$$

where $\Delta f = 1/\tau_{on}$. The one-sided spectral density of $y(t)$ is computed by adding the squares of the real and imaginary components of Y and dividing by the duration τ_{on} of the data run:

$$S_y(m\Delta f) = 2\frac{\{R[Y(m\Delta f]\}^2 + \{I[Y(m\Delta f]\}^2}{\tau_{on}} \qquad \text{Eq. 6}$$

with BW = 1 Hz and RBW = Δf. Converting to L(f), one uses **[6]**:

$$L(m\Delta f) = \frac{1}{2}S_\phi(m\Delta f) = \frac{1}{2}\frac{\nu_0^2}{(m\Delta f)^2}S_y(m\Delta f) \qquad \text{Eq. 7}$$

and L(f) is plotted on log-log scales.

In practice, the noise of each limited-live spectrum affects Doppler-track error. Averages of limited-live estimates of L($m\Delta f$) are shown in Fig. 7 for the OCXO and TCXO. A word of caution—L(f) derived from fast-frequency measurements in setup Fig. 1 will not be sensitive to white and flicker PM noise, as mentioned earlier. This is not problematic to most limited-live characterizations, because the measurement high-frequency cutoff (BW) is $f_c = 1/(2\pi\tau_0)$, and τ_0 is of the order 10^{-3} in this case. Thus L(f) is not computed beyond f of several hundred hertz, even in the best case.

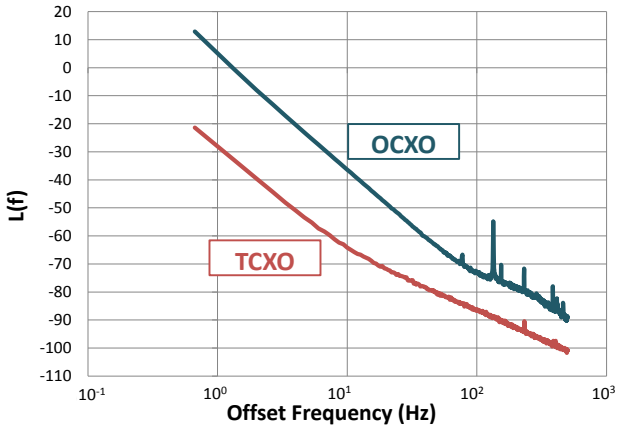

Figure 7. L(f) for the OCXO and TCXO from dead-time measurements.

For future studies, characterization of limited-live oscillators in this paper will be used while such oscillators are subject to temperature and vibration stresses.

REFERENCES

[1] D.A. Howe, 2006, *"ThêoH: a hybrid, high-confidence statistic that improves on the Allan deviation,"* **Metrologia**, **vol. 43**, S322-S331, BIPM and IOP, UK.

[2] L. Galleani and P. Tavella,2005, *"Tracking Nonstationarities In Clock Noises Using the Dynamic Allan Variance,"* FCS/PTTI, August 2005,Vancouver, British Columbia, Canada, pp. 392-396.

[3] J.A. Taylor and D.A. Howe, 2009, *"Fast TheoBR: A Method for Long Data Set Stability Analysis,"* **IEEE T. Ultrason. Ferr., vol. 57**, no. 9, pp. 2091-2094, Sept. 2009.

[4] J. Levine, 1999, *"Introduction to Time and Frequency Metrology,"* **Review of Scientific Instruments**, **Vol. 70**, pp. 2567-2596.

[5] D.W. Allan, 1966, "*Statistics of Atomic Frequency Standard*," **IEEE Proc.**, **vol. 54**, No. 2, 221-231.

[6] D.A. Howe, D.W. Allan, and J.A. Barnes, 1981, *"Properties of Signal Sources and Measurement Methods,"* Proc. 35th Annual Symp. on Freq. Control.

[7] J.A. Barnes, 1969, *"Tables of Bias Functions, B_1 and B_2, for Variances Based on Finite Samples of Processes with Power Law Spectral Densities,"* NBS Technical Note 375, Jan. 1969.

[8] P. Lesage, 1983, *"Characterization of Frequency Stability: Bias Due to the Juxtaposition of Time-Interval Measurements,"* **IEEE Trans. Instrum. Meas., Vol. IM-32**, No. 1, 204-207, March 1983.